Annuaire de l'Université "St. Kliment Ohridski", Faculté de Physique, 98, 2005

DIFFRACTION FROM MONOLAYER LATEX CRYSTALS

NATALIA DUSHKINA*, CECO DUSHKIN, KUNIAKI NAGAYAMA**

Department of General and Inorganic Chemistry, Faculty of Chemistry
**Department of Physics and Astronomy, Bowling Green State University, USA*
***Okazaki Institute for Integrative Bioscience,*
National Institute of Natural Sciences, Japan

Наталия Душкина, Цецо Душкин, Куниаки Нагаяма. ДИФРАКЦИЯ ОТ МОНОСЛОЙНИ ЛАТЕКСНИ КРИСТАЛИ

Тук ние измерваме дифракционната ефективност на решетка, състояща се от двумерен латексен кристал върху стъклена подложка. Микронните по размер сферични частици са нанесени в монослойна решетка с хексагонална опаковка, използвайки изсъхваща капка от водна суспензия върху подложката. Дифракционната ефективност е измерена в планарна геометрия, когато лъч пада върху латексния филм откъм въздуха, и в геометрията на пълно вътрешно отражение (ПВО), когато лъчът пада върху латексната решетка през стъклена призма в оптичен контакт с подложката. В планарна геометрия експерименталните криви показват забележими максимуми и минимуми поради комплексното поведение на дифракцията от различен порядък, зависещ от поляризацията на светлината. Интензитетът на отразената светлина (нулев дифракционен порядък) със s- и p-поляризация има минимум при ъгъл от около 53°, аналог на ъгъла на Брюстер, откъдето ние изчисляваме коефициента на пречупване на диелектричния филм от частици $1,32$. Интензитетът на преминалата светлина минава през максимум, по-добре очертан за p-поляризирана светлина, разкриващ преноса на енергия от първия дифракционен порядък. Светлинните петна за първия дифракционен порядък, две по две, имат или идентично, или подобно поведение и могат да бъдат групирани в двойки, които изчезват при определен ъгъл поради пренос на енергията към другите, все още съществуващи порядъци. В геометрията на ПВО се наблюдават силни промени в дифракционните ефективности на всички порядъци в близост до критичния ъгъл.

Natalia Dushkina, Ceco Dushkin, Kuniaki Nagayama. DIFFRACTION FROM MONOLAYER LATEX CRYSTALS

Here we measure the diffraction efficiency of a grating comprising a two-dimensional latex crystal on a glass substrate. The micron sized spherical particles are deposited in a monolayer array of hexagonal packing using a drying water suspension droplet on the substrate. The diffraction efficiency has been measured in planar geometry, when the incident beam of light strikes the latex film from the air side, and in geometry of Total Internal Reflection (TIR), when the beam falls onto the latex array through a glass prism coupled to the substrate. In planar geometry, the experimental curves exhibit peculiar maxima and minima due to the complex behavior of the diffraction of different order depending on the polarization of light. The intensity of reflected light (zeroth diffraction order) of s- and p-polarization has a minimum at an angle of about 53°, an analog to the Brewster angle, from where we calculate the refractive index of the dielectric particle film 1.32. The intensity of transmitted light passes through a maximum, better pronounced for p-polarized light, implying on the transfer of energy from the first diffraction order. The light spots for the first diffraction order, two by two, have either identical or similar behavior and can be grouped in couples which vanish at a determined angle with the energy transferred to the other still existing orders. In TIR geometry, strong changes in the diffraction efficiencies of all orders are observed near the critical angle.

Keywords: diffraction grating, 2D-latex array, colloidal crystal, total internal reflection

PACS numbers: 42.25.Fx, 42.79.Dj, 42.79.Gn, 81.16.Dn

1. INTRODUCTION

The geometry of Total Internal Reflection (TIR) is important for applications in waveguide optics and integral optics. Diffraction gratings working in TIR geometry exhibit peculiarities in the diffraction efficiency of different orders, which makes it possible the controllable concentration of light energy in one diffraction order different from the zeroth order. Planar or 1D-diffraction gratings have been widely studied, because of their applications as deflectors of light in waveguide optics. The special case of metal diffraction gratings consisting of metal stripes on a glass substrate obtained by holographic recording, were investigated in details in [1,2], where the experimental data were compared with the theoretical predictions obtained by using the Fraunhofer's approximation of the scalar diffraction theory. If these metal diffraction gratings work in a regime of Total Internal Reflection of the incident light, the scalar theory could be applied and the behavior of the diffraction efficiency in zeroth and first order could be described with two relatively simple equations, derived in [2] for transmitted and reflected lights, respectively.

An alternative of the considered "physical" diffraction gratings are the "colloidal" gratings comprising two-dimensional (2D) arrays of latex particles which are known since long ago [3–6] (for a recent review see Ref. [7]). Alfrey, Jr., et al. [3] have shown that the scattering of light by transparent films of poly(vinyltoluene) particles of diameters d from 0.165 to 0.986 μm is due to the Fraunhofer diffraction from independent spheres. They have measured the diffraction angle θ_{d} at different

wavelengths as a function of the specimen orientation angle δ. The expression $m\lambda/\Lambda = 2\sin^2(\theta_d/2) - \delta\sin\theta_d$, derived by them for an one-dimensional (1D) chain of scatterers, explains the linear relationship between θ_d and δ (m is an integer, Λ is the spacing between particles, λ is the wavelength of incident light). Krieger and O'Neill [4] have studied the diffraction from 2D-crystals of poly(vinyltoluene) latex particles of diameters d ranging from 0.1825 to 3.075μm. They have found diffraction patterns in the form of concentric circular rings for a polycrystalline array and single spots, located at the corners of concentric hexagons, for a monocrystalline array. They have generalized the theoretical approach from Ref. [3] for a two-dimensional scattering array $m\lambda/\Lambda = (\sqrt{3}/2)(\sin\theta_1 + \sin\theta_2)$, where θ_1 and θ_2 are the angles of incidence and diffraction, respectively. Both studies [3,4] utilize a planar geometry of diffraction (for a definition see below) which is not compatible to the waveguide optics.

Recently, the nano-world phenomena became rather popular, and in this context, the opportunity to build 2D-diffraction gratings using spherical micro- or nano-sized particles in monolayer thin films brings new horizons for investigations and applications. Accessing the nanoparticle range necessarily goes first through the use of micron sized particles with respect to the way of their self-assembly [6]. Similarly, approaching the optical properties of the 2D-nanoarrays one should also use first micrometer in size particles.

This paper is devoted to the diffraction properties of a 2D-latex crystal of polystyrene particles in both planar geometry and TIR geometry. The monolayer crystal is illuminated with a monochromatic laser light of defined polarization. The effect of the polarization state of the incident light on the intensities of reflected and transmitted lights is revealed and compared for the basic diffraction orders as a function of the incident angle. The 2D-latex crystal grating might be used for coupling light into an optical fiber with a hexagonal structure.

2. SAMPLE PREPARATION

The latex monocrystal, shown in Fig. 1a, is colored due to the diffraction of white light from the domains of ordered particles. These domains, exhibiting different colors, are of varying crystalline structure, size and orientation, reflecting the conditions of crystal growth. The 2D-crystal is grown, using known procedures [6,7], on a glass substrate in a circular Teflon cell of diameter 14 mm, tightly attached to the glass surface. The cell is loaded with a latex suspension in water (suspension volume 25μl) with a particle diameter $d = 1.696\mu$m (JSR Co.) and a particle volume fraction of 0.01. The water is allowed to evaporate from the suspension at controlled air humidity until a micron thin film is formed in the central portion of the cell. At this moment the latex particles, protruding from the film surface, form locally curved menisci conducting the capillary interaction between two neighboring particles [6]. This triggers the formation of a dense particle array which plays further the role of a monolayer nucleus for the crystal growth. This nucleus of a nearly circular shape, located at the central portion of

the monocrystal, is composed of smaller in size domains. It loses water due to the evaporation from its surface for which reason new water is coming from the surrounding suspension in replenishment. The water flow is bringing latex particles which tightly attach to the circumference thus increasing the crystal size in a radial direction. The respective domains become bigger seen as blue and green stripes. A sort of capillary instability causes the formation of a particle bilayer appearing as the dark rings surrounding the monolayer.

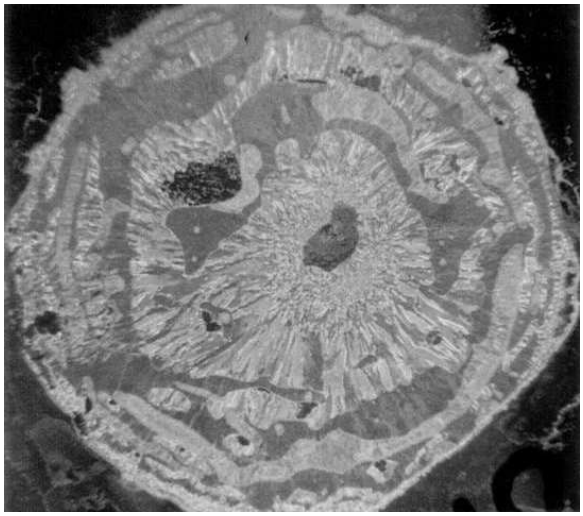

(a)

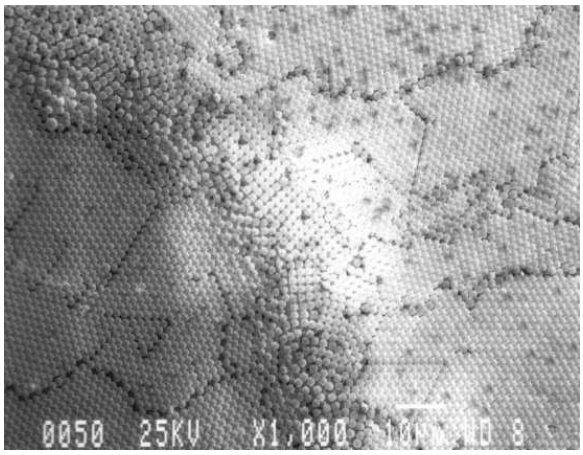

(b)

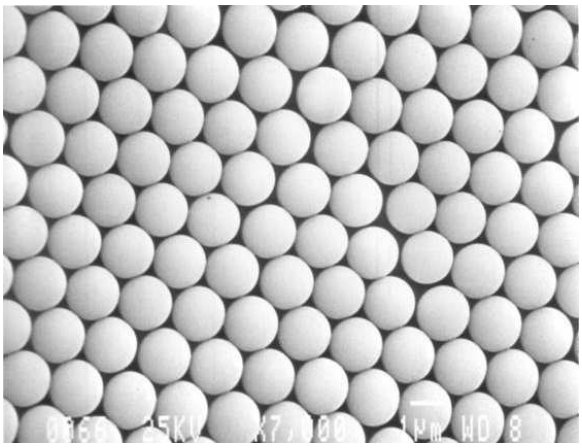

(*c*)

Fig. 1. Two dimensional crystal of micron size latex particles: (*a*) General view of a crystal of latex particles grown on a transparent plate (crystal diameter 1.4 cm); (*b*) Boundary between a monolayer (left) and bilayer (right) of latex spheres of diameter 1.696μm. Magnification: $\times$1000; (*c*) Magnified part of the crystal monolayer with ordered latex spheres (magnification $\times$7000)

The close examination of the crystal structure with Scanning Electron Microscope (SEM) shows that the monolayer and bilayer are of general hexagonal packing separated by tetragonal packed bilayer in between (Fig. 1*b*). Also seen are the dislocations separating two neighboring domains of ordered particle rows. These domains produce the diffraction colors in white light in Fig. 1*a*. In our diffraction experiments we probe with the laser beam several different points of the monolayer crystal. Each point may spread on more than one particle domain. Figure 1c shows the high precision of local hexagonal ordering in the monolayer which seems dominating the diffraction orders thereafter. A dry 2D-latex crystal remains stable on the substrate for several years.

The 2D-latex crystal is grown prior to the optical experiments on a glass substrate (glass K-8, with a refractive index n_1=1.514 at λ=632.8 nm). The refractive index of bulk polystyrene is given as [5]

$$n_2^b(\lambda) = 1.5683 + 1.0087 \times \frac{10^4}{\lambda^2}\,, \tag{1}$$

where λ is in nm. From here n_2^b=1.59349 at λ=632.8 nm. The refractive index of the monolayer will depend on the film volume fraction of particles Φ, $n_2(\Phi) = n_2^b\Phi + n_3(1-\Phi)$ [5, 8]. Here $(1-\Phi)$ is the volume fraction of air voids of refractive index n_3=1 in the film. For hexagonal packing $\Phi = 0.6046$ [8], which gives in turn $n_2 = 1.35882$.

3. EXPERIMENT

In order to compare the behavior of the different diffraction orders in planar and TIR geometry of the incident light, and on this base to reveal the peculiarities of the diffraction efficiency in TIR geometry, we used two experimental arrangements to measure the intensity of the different diffraction orders (Fig. 2). In the case of planar geometry, shown in Fig. 2*a*, the incident monochromatic light strikes the sample from the air side, while in the case of TIR geometry in Fig. 2*b* the light falls onto the 2D-latex crystal through a glass prism. The source of monochromatic light is a He-Ne laser (Spectra-Physics 136P) with an output power 2 mW at a wavelength λ=632.8 nm. A rotator controls the polarization of the light falling on the sample. We measured the diffraction efficiency for both cases of polarization: when the incident light is perpendicular (s-polarization) and parallel to the plane

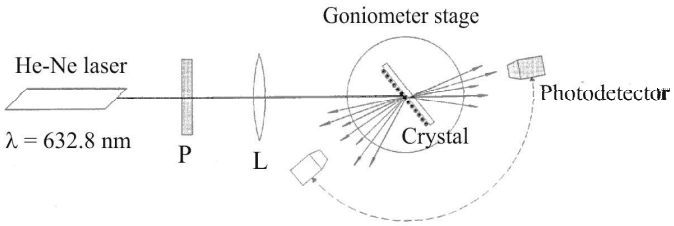

(*a*)

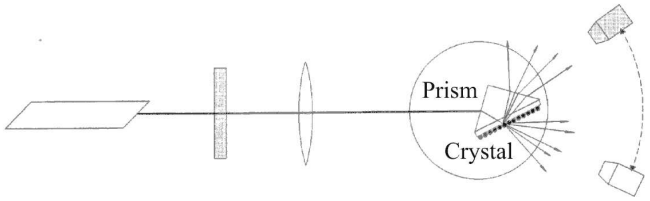

(*b*)

Fig. 2. Experimental setup to measure the diffraction from 2D-crystals of latex particles in: (*a*) arrangement of planar geometry; (*b*) arrangement of Total Internal Reflection (TIR) geometry

of incidence (p-polarization). The glass substrate with the 2D-latex crystal is in optical contact with a TIR isosceles prism that has a refraction angle of 45°. The prism is made of the same type of glass as the substrate ($n_1 = 1.514$). The glass prism, with investigated sample on it, is mounted on a rotary table (Microcontrole

TR80), which defines the incident angle θ_0. In the case of planar geometry, this is directly the angle at which the light hits the 2D-crystal. For TIR geometry, θ_0 is the angle at which the light strikes the input wall of the prism and from which the angle of incidence on the crystal θ is calculated. The accuracy of measuring the external angle θ_0 is $1'$. The angle θ_0 varies in the working range 0–70° for the planar case, and from $-25°$ to $+15°$, corresponding to internal angles θ from 28° to 55° for the TIR case.

The incidence angle θ, under which the light hits the 2D-crystal through the prism, is calculated using the relation:

$$\theta = \alpha \pm \sin^{-1}\left(\frac{\sin\theta_0}{n_1}\right), \tag{2}$$

where $\alpha = 45°$ is the refractive angle and n_1 is the refractive index of the prism. The light intensity is measured with a precise photometer-radiometer Ealing-910 with a sensitivity of 10^{-9} W cm^{-2}. Thus, the maximum relative error of the measurements is 3%.

The intensities of the different diffraction orders $I_{\rm m}$ are measured as a function of the incident angle θ, and the diffraction efficiency $\eta_{\rm m}$ is determined from the ratio $\eta_{\rm m} = I_{\rm m}/I_{\rm inc}$, where $I_{\rm inc}$ is the intensity of the light incident on the prism.

4. RESULTS AND DISCUSSION

The photograph of the diffraction pattern observed from the latex monolayer in a monochromatic laser light (planar geometry) is given in Fig. 3a. Figure 3b shows a reconstruction of the spots with the diffraction orders marked with numbers mj for easy consideration. In the center is the zeroth order m=0, around which are symmetrically distributed the higher diffraction orders. The hexagonal symmetry of the 2D-crystal is reproduced by the diffraction pattern, produced by the monolayer. Each diffraction order $m = 1, 2, \ldots$ consists of six spots circling the zeroth order, which are numbered $j = 1, 2, \ldots, 6$. At normal incidence, the diffraction pattern is symmetrical and the intensity decreases for the higher diffraction orders—the higher the number of diffraction order, the lower the intensity of diffracted light in it. The diffraction pattern changes with the polarization and the incident angle θ. The zeroth order follows the path of the incident transmitted or reflected light. The six spots of first and higher orders differ from each other and, due to the circular symmetry of the pattern, are grouped in three couples. The transmitted and reflected spot couples vanish one by one, and the diffraction angle θ_{mj} at which the m-th order subsides, can be determined from the equation of the diffraction grating [9]:

$$\frac{m\lambda}{\Lambda} = n_3 \sin\theta_{mj} - n_1 \sin\theta, \qquad m = 0, \pm1, \pm2, \ldots, \quad j = 1, 2, \ldots, 6. \tag{3}$$

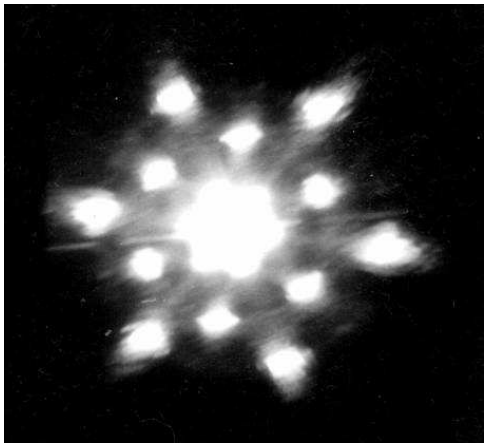

(*a*)

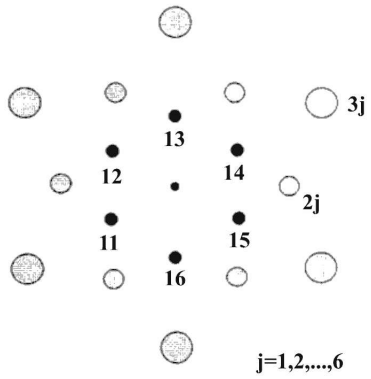

(*b*)

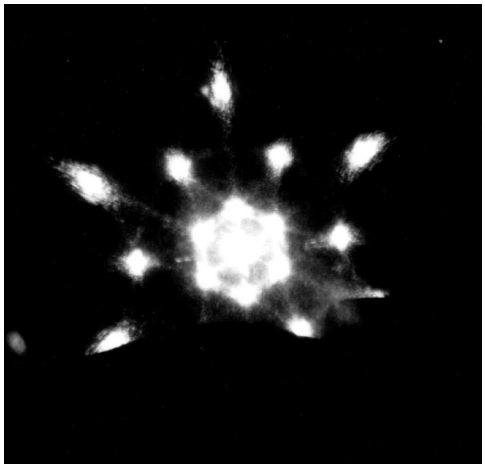

(*c*)

Fig. 3. Typical diffraction patterns observed from the latex monolayer in monochromatic light: (*a*) Photograph of the experimental patterns in planar geometry; (*b*) Reconstruction of the spots with marked diffraction orders; (*c*) Photograph of the experimental patterns in TIR geometry

Here n_1 and n_3 are the refractive indices of the media on both sides of the 2D-latex crystal (in planar geometry, the substrate with the latex crystal is in air, thus, $n_3 = 1$), Λ is the period of the diffraction grating and $\lambda = 632.8$ nm is the wavelength of the incident light. In our case, we have one and the same grating spacing in both directions, which is the reason for the circular symmetry and the

grouping of the spots in couples. For a two-dimensional grating with two different grating spacing in x- and y-directions, two equations should be considered. Similar trends can be observed for the diffraction patterns in TIR geometry (Fig. 3c).

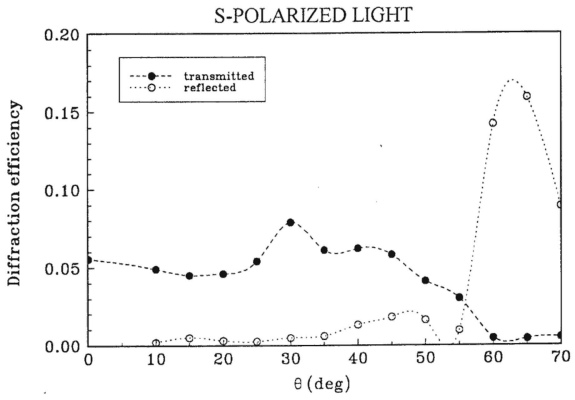

(a)

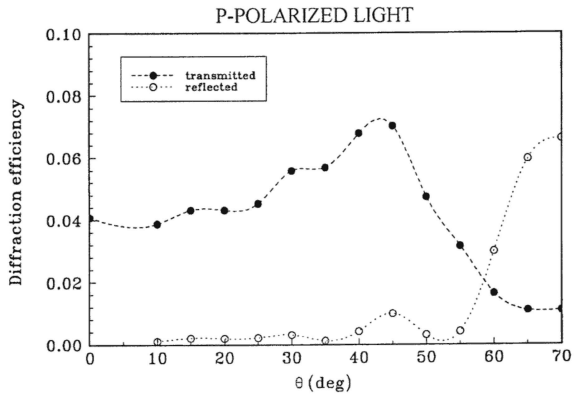

(b)

Fig. 4. Diffraction efficiency of the latex crystal grating in the zeroth order in a planar geometry: (a) s-polarized incident light; (b) p-polarized incident light

Figure 4 represents the diffraction intensity of the latex crystal grating in the basic (zeroth) order in planar geometry: (a) for s-polarized light and (b) for p-polarized light. The measurements for reflected light are given with empty circles, and those for transmitted light—with solid circles. In general, the zeroth order in transmitted and reflected light follows the common behavior of transmission and reflection through an optical boundary [9]. Similar is the behavior also of linear metal diffraction gratings, consisting of regular metal stripes deposited on a glass

substrate [1]. The intensity of reflected light for both polarizations is very weak (below 1%) for angles up to 55°, and increases at larger angles due to the glancing incidence. There is a weak maximum observed in both curves in the vicinity of 40–50° (Fig. 4*a* and *b*, empty circles) that might be explained with a transfer of energy from the first orders s_{14}, s_{15}, p_{14}, p_{15} in reflected light, which attenuate at angles about 40°. The following minimum at 50–55° is an analog of the angle of Brewster, $\varphi = \arctan(n_2)$. If we calculate the refractive index of the latex crystal for the Brewster angle $\varphi = 54°$, the value would be $n_2 \sim 1.32$, which is reasonable, because of the filling factor of the layer—spherical particles with refractive index of about 1.59 and air of index 1.0 between them. This value of n_2 is rather close to the refractive index for a layer of closely packed polystyrene particles calculated above ($n_2 = 1.36$) and mentioned in Ref. [8] ($n_2 = 1.4$).

This finding opens a new application of our method to measure the refractive indices of thin particle films. If the experiment is precise enough and the angle is measured only in the vicinity of the Brewster angle for p-polarization, one can determine the refractive index of a thin dielectric film of spherical particles which is difficult to be calculated, because of the multilayer and domain structure and defects making the density irregularly distributed. Our method is much simpler than the surface plasmon resonance method used recently for a similar purpose [10].

The measured diffraction efficiency of transmitted light is in the order of few percents for both polarizations, and strongly decreases at angles above 50°. As the reflected light, both curves go through a maximum (more pronounced for p-polarization) in the vicinity of 40–50° (Fig. 4*a* and 4*b*, solid circles) connected with a transfer of energy from the first orders s_{14}, s_{15}, p_{14}, p_{15} in transmitted light, which attenuate at angles about 35–40°. At normal incidence ($\theta = 0°$), the pattern is symmetrical, and as it might be expected from a theoretical description using Bessel functions, the zeroth transmitted order, corresponding to the straight transmitted light, has the highest intensity—about 5% for s-polarization of incident light and 4% for p-polarization. The next first diffraction order contains about 1% less energy than the zeroth order for both polarizations, respectively, as the total energy concentrated in zeroth and first order only is about 53%. The remaining part is distributed in the higher transmitted and reflected orders.

Still considering the planar geometry of incident light, the distribution of the intensity in the spots of first diffraction order is shown in Fig. 5 for: (*a*) transmitted s-polarization; (*b*) reflected s-polarization; (*c*) transmitted p-polarization; and (*d*) reflected p-polarization. It is clearly seen that two by two the light spots have identical (in some cases) or similar (in other cases) behavior and can be grouped in couples. Each couple vanishes at a determined angle, e.g., both couples s_{14}, s_{15}, and p_{14}, p_{15} for both transmitted and reflected light disappear at an incident angle of about 40°, while the central couples s_{13}, s_{16}, and p_{13}, p_{16}—at an incidence angle around 60°, which corresponds to the angles calculated using the equation of the diffraction grating. (For this purpose, one should assume an efficient diffraction grating of period $\Lambda \sim 950$ nm, which is about half of the latex particle diameter). The energy of the vanished orders is transferred to the other still existing orders,

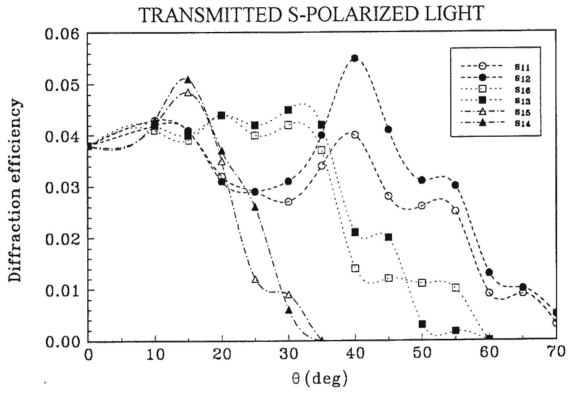
TRANSMITTED S-POLARIZED LIGHT
Diffraction efficiency
θ (deg)
S11
S12
S16
S13
S15
S14

(*a*)

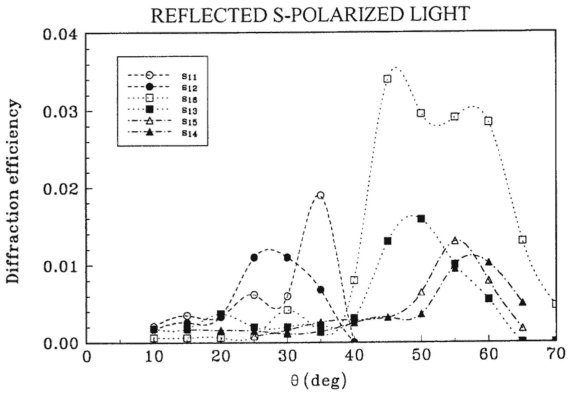
REFLECTED S-POLARIZED LIGHT
Diffraction efficiency
θ (deg)
S11
S12
S16
S13
S15
S14

(*b*)

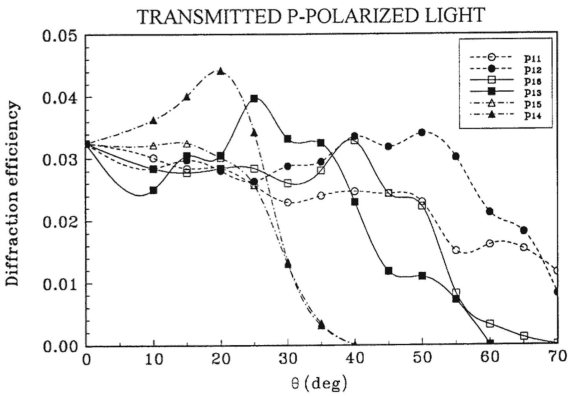
TRANSMITTED P-POLARIZED LIGHT
Diffraction efficiency
θ (deg)
P11
P12
P16
P13
P15
P14

(*c*)

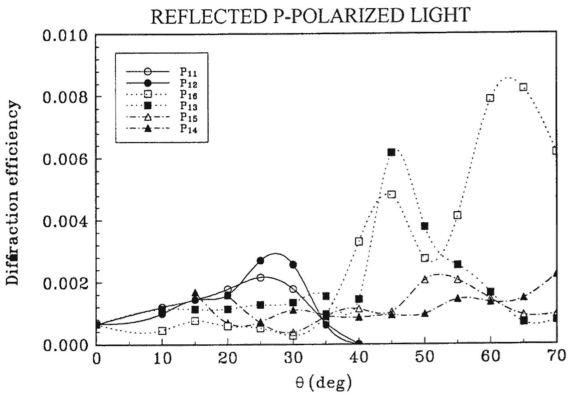

(*d*)

Fig. 5. Diffraction efficiency of the latex crystal grating in the first order in a planar geometry: s-polarized incident light: (*a*) transmitted diffraction light; (*b*) reflected light. P-polarized incident light; (*c*) transmitted diffraction light; (*d*) reflected light

which explains their fluctuating behavior and the presence of maxima around the angles of disappearance of the vanishing orders. Such study of the diffraction efficiency might be very useful for evaluation of the optical losses, when a 2D-structure of spherical micro-particles is used as a diffraction grating for coupling light into a hexagonal fiber structure (e.g., an optical cable).

In the case of TIR geometry, the behavior of the diffraction orders is related to the critical angle θ_c

$$\theta_c = \sin^{-1}\left(\frac{n_3}{n_1}\right). \tag{4}$$

Here the refractive indices of the media on both sides of the 2D-latex crystal n_1 and $n_3 = 1$ are different ($n_1 > n_3$). Near the critical angle of TIR ($\theta_c = 41°20'$) strong changes in the diffraction efficiencies of all orders are observed. The transmitted orders disappear in the vicinity of the critical angle and their energy is transferred into the existing orders of reflected light. Figure 6 shows the measured diffraction efficiency in reflected light as follows: (*a*) zeroth order and (*b*) second order. The dependence of the diffraction efficiency of the zeroth reflected order on the angle of incidence reminds very much the behavior of the zeroth diffraction order from planar metal diffraction gratings (compare with Fig. 2 from [2]). This fact suggests that the scalar diffraction theory in Fraunhofer's approximation might be used for a rough description of the behavior of the zeroth order. The well pronounced maximum for p-polarization in the vicinity of the critical angle, in which the diffraction efficiency reaches about 10%, could be used for characterization of the 2D-crystal, especially in the monolayer domains. Due to internal reflections in the prism, as well as to the TIR geometry of the experiment, not all the spots of the first and higher orders could be observed and accurately

measured (see Fig. 3*c*). Therefore, only four spots of second reflected order are illustrated in Fig. 6*b*. The behavior of the second order also reminds the one of a grating consisting of metal stripes on a dielectric substrate (compare with Fig. 4 from [2])—the curves for both polarizations pass through a maximum in the vicinity of the critical angle. Although, the maximum diffraction efficiency measured in spots p_{22} and p_{23} is only about 2%, the maxima are very well pronounced and, as in the case of zeroth order, could be used for characterization of the 2D-crystal.

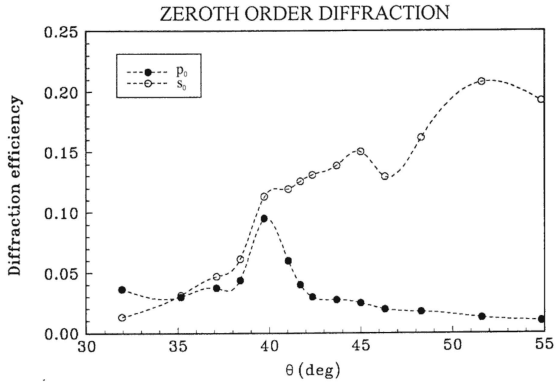

(*a*)

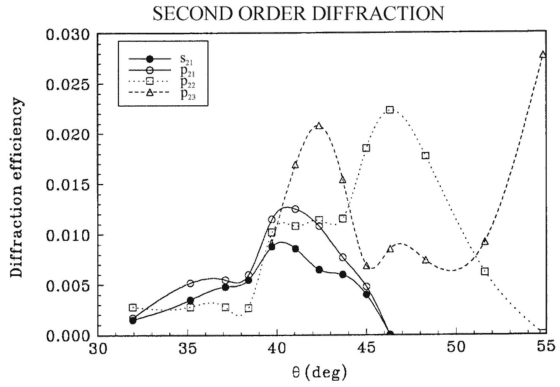

(*b*)

Fig. 6. Diffraction efficiency of the latex crystal in TIR geometry (s- and p-polarized incident light): (*a*) zeroth order diffraction; (*b*) second order diffraction

The geometrical positions of diffraction spots observed by us in both planar and TIR arrangement should obey the conditions for Bragg diffraction described in Ref. [3] for 1D-grating and generalized in Ref. [4] for 2D-grating of hexagonal

packing. Here we pay more attention to the intensity of light in different diffraction orders, which is important for the implication of latex gratings in the fiber optics for wave-guiding. The calculation of diffracted light intensity, which was not achieved by the authors of [3,4], would explain the transfer of light energy between different diffraction orders revealed in our study. The reflected light intensity has been calculated for a 2D-array of random latex particles based on the Mie scattering theory for non-correlated spheres [11,12]. For ordered close packed spheres in a diffraction grating one should correlate the scatterers using either the Raman-Nath approach [9] or the theory for amplitude and phase diffraction gratings [2]. In both cases one should generalize the respective equations: first, for the diffraction from 1D-grating of close packed semicircles and second, for hemispheres in a 2D-hexagonal array.

Our findings here for the diffraction from a dry "colloidal" grating can be applied also for a slab of a wet colloidal crystal, which was found to obey Bragg diffraction for both aqueous [5,13] and non-aqueous [14] concentrated suspensions of latex particles.

5. CONCLUSIONS

The peculiarities in the behavior of the diffraction efficiency of 2D-latex crystal gratings were investigated in planar geometry, when the light strikes the crystal through air, and in TIR geometry, when the light impinge on the crystal through a glass prism. The behavior of the diffracted orders in planar geometry, though much more complicated, follows the general tendency of the common transmission and reflection from a boundary between two dielectric media. The behavior of the diffraction orders in reflected light in TIR geometry, reminds the behavior of zeroth and second order of a plane metal diffraction grating, which was well described in [2] by Fraunhofer's approximation of the scalar diffraction theory. Our method can be applied to measure the refractive index of thin dielectric films of nanoparticles. The latex crystal diffraction gratings, based on their long-term stability and brilliant optical properties, can be utilized for coupling of light into a hexagonal fiber structure like an optical cable.

Acknowledgement: This research has been supported financially by the Program ERATO of the Research and Development Corporation of Japan (JRDC) in the frames of the Nagayama Protein Array Project.

REFERENCES

1. Spasova, E., B. Mednikarov, G. Danev, S. Sainov, N. Dushkina. Proc. Holography'89. *SPIE*, **1183**, 1989, 683.
2. Dushkina, N., S. Sainov. *J. Mod. Optics,* **39**, 173 (1992).
3. Alfrey, Jr., T., E. B. Bradford, J. W. Vanderhoff, G. Oster. *J. Opt. Soc. Am.,* **44**, 1954, 603.
4. Krieger, M., F. M. O'Neill. *J. Am. Chem. Soc.,* **90**, 1968, 3114.

5. Goodwin, J. W., R. H. Ottewill, A. Parentich. *J. Phys. Chem.,* **84**, 1980, 1580.
6. Denkov, N. D., O. D. Velev, P. A. Kralchevsky, I. B. Ivanov, H. Yoshimura, K. Nagayama. *Langmuir,* **8**, 1992, 3183.
7. Dushkin, C., G. S. Lazarov, S. N. Kotsev, H. Yoshimura, K. Nagayama. *Colloid Polym. Sci.,* **277**, 1999, 914.
8. Dushkin, C. D., K. Nagayama, T. Miwa, P. A. Kralchevsky. *Langmuir,* **9**, 1993, 3695.
9. Born, M., E. Wolf. Principles of Optics. Oxford, Pergamon Press, 1970.
10. Kotsev, S. N., C. D. Dushkin, I. K. Ilev, K. Nagayama. *Colloid Polym. Sci.,* **281**, 2003, 343.
11. Koper, G. J. M., P. Schaaf. *Europhys. Lett.*, **22**, 1993, 543.
12. Mann, E. K., E. A. van der Zeeuw, G. J. M. Koper, P. Schaaf, D. Bedeaux. *J. Phys. Chem.*, **99**, 1995, 790.
13. Hiltner, P. A., I. M. Krieger, *J. Phys. Chem.,* **73**, 1969, 2386.
14. Hiltner, P. A., Y. S. Papir, I. M. Krieger, *J. Phys. Chem.,* **75**, 1971, 1881.

Received August 2004

Natalia Dushkina
Department of Physics and Astronomy
College Physics, 104 Overman Hall
Bowling Green State University
Bowling Green, OH 43402, USA
E-mail: natalie@kottan-labs.bgsu.edu

Ceco Dushkin
St. Kliment Ohridski University of Sofia
Faculty of Chemistry
Group of Nanoparticle Science and Technology
Department of General and Inorganic Chemistry
1 James Bourchier Blvd., 1164 Sofia, Bulgaria
E-mail: nhtd@wmail.chem.uni-sofia.bg

Kuniaki Nagayama
Okazaki Institute for Integrative Bioscience
National Institutes of Natural Sciences
5-1, Higashiyama, Myodaiji-cho, Okazaki
Aichi 444-8787, Japan
E-mail: nagayama@nips.ac.jp